NAVAL AIR WARFARE CENTER AIRCRAFT DIVISION
PATUXENT RIVER, MARYLAND

TECHNICAL REPORT

REPORT NO: NAWCADPAX/TR-2012/365

INVESTIGATION OF AEROSOL PENETRATION THROUGH INDIVIDUAL PROTECTIVE EQUIPMENT IN ELEVATED WIND CONDITIONS

by

Mr. Michael A. Hill
Dr. Suresh Dhaniyala
Mr. Terence A. Ghee
Dr. Jonathan Kaufman

1 March 2013

Approved for public release; distribution is unlimited.

DEPARTMENT OF THE NAVY
NAVAL AIR WARFARE CENTER AIRCRAFT DIVISION
PATUXENT RIVER, MARYLAND

NAWCADPAX/TR-2012/365
1 March 2013

INVESTIGATION OF AEROSOL PENETRATION THROUGH INDIVIDUAL PROTECTIVE EQUIPMENT IN ELEVATED WIND CONDITIONS

by

Mr. Michael A. Hill
Dr. Suresh Dhaniyala
Mr. Terence A. Ghee
Dr. Jonathan Kaufman

RELEASED BY:

Steven A Donaldson 1 Mar 2013
STEVEN A. DONALDSON / AIR-4.3.2 / DATE
Head, Aeromechanics Division
Naval Air Warfare Center Aircraft Division

REPORT DOCUMENTATION PAGE

Form Approved
OMB No. 0704-0188

1. REPORT DATE	2. REPORT TYPE	3. DATES COVERED
1 March 2013	Technical Report	March 2004 – December 2012

4. TITLE AND SUBTITLE

Investigation of Aerosol Penetration through Individual Protective Equipment in Elevated Wind Conditions

5a. CONTRACT NUMBER

5b. GRANT NUMBER

5c. PROGRAM ELEMENT NUMBER

6. AUTHOR(S)

Mr. Michael A. Hill
Dr. Suresh Dhaniyala
Mr. Terence A. Ghee
Dr. Jonathan Kaufman

5d. PROJECT NUMBER

5e. TASK NUMBER

5f. WORK UNIT NUMBER

7. PERFORMING ORGANIZATION NAME(S) AND ADDRESS(ES)

Naval Air Warfare Center Aircraft Division
22347 Cedar Point Road,
Patuxent River, Maryland 20670-1161

8. PERFORMING ORGANIZATION REPORT NUMBER

NAWCADPAX/TR-2012/365

9. SPONSORING/MONITORING AGENCY NAME(S) AND ADDRESS(ES)

Naval Air Systems Command
Patuxent River, Maryland 20670-1547

10. SPONSOR/MONITOR'S ACRONYM(S)

11. SPONSOR/MONITOR'S REPORT NUMBER(S)

12. DISTRIBUTION/AVAILABILITY STATEMENT

Approved for public release; distribution is unlimited.

13. SUPPLEMENTARY NOTES

14. ABSTRACT

A methodology to characterize particle penetration characteristics of individual protective equipment (IPE) under elevated wind conditions is developed. Performance of a complete IPE system can be determined from the knowledge of the performance characteristics of the IPE subsystems or components. Here, particle penetration characteristics of a cylindrical-shaped component, consisting of an outer fabric sleeve enclosing an inner appendage, are studied as a function of particle size and ambient wind conditions. A component particle penetration model is developed by combining a potential flow model to calculate flow through and around a component with a filtration model. The filtration model combines classical filtration theory with simple bench top experiments to determine net particle penetration. The component model predictions of particle penetration through a cylindrical component suggest that its filtration performance is strongly dependent on particle size and ambient wind velocities. To test model predictions, wind tunnel experiments are conducted over an ambient wind velocity range of 10-80 mph (5 to 40 ms^{-1}) and particle diameter range of 10 nmi to 2 μm. The experimental results validate model predictions of particle penetration through a cylindrical component. The component model can be extended to model the integrated IPE system considering it to be composed of a combination of cylindrical components.

15. SUBJECT TERMS

Individual Protective Equipment (IPE); Aerosol Penetration

16. SECURITY CLASSIFICATION OF:			17. LIMITATION OF ABSTRACT	18. NUMBER OF PAGES	19a. NAME OF RESPONSIBLE PERSON
a. REPORT	b. ABSTRACT	c. THIS PAGE			Terence Ghee
Unclassified	Unclassified	Unclassified	SAR	36	19b. TELEPHONE NUMBER (include area code) (301) 342-8536

Standard Form 298 (Rev. 8-98)
Prescribed by ANSI Std. Z39-18

SUMMARY

A methodology to characterize particle penetration characteristics of individual protective equipment (IPE) under elevated wind conditions is developed. Performance of a complete IPE system can be determined from the knowledge of the performance characteristics of the IPE subsystems or components. Here, particle penetration characteristics of a cylindrical-shaped component, consisting of an outer fabric sleeve enclosing an inner appendage, are studied as a function of particle size and ambient wind conditions. A component particle penetration model is developed by combining a potential flow model to calculate flow through and around a component with a filtration model. The filtration model combines classical filtration theory with simple bench top experiments to determine net particle penetration. The component model predictions of particle penetration through a cylindrical component suggest that its filtration performance is strongly dependent on particle size and ambient wind velocities. To test model predictions, wind tunnel experiments are conducted over an ambient wind velocity range of 10-80 mph (5 to 40 ms^{-1}) and particle diameter range of 10 nmi to 2 μm. The experimental results validate model predictions of particle penetration through a cylindrical component. The component model can be extended to model the integrated IPE system considering it to be composed of a combination of cylindrical components.

Contents

ACKNOWLEDGEMENTS

The authors wish to thank the Defense Threat Reduction Agency, JSTO CB/CBT for providing funding for this work (DTRA Agreement No. SEA 139). In addition, we acknowledge the invaluable support of J. J. Armstrong at RED, Inc.; Jim Hanley at RTI, International; and Tom Cao, Jim Hanzelka, Andrew Neafsey, and Richard Phan at Dugway Proving Ground.

INTRODUCTION

To protect against harmful aerosols, any air-permeable protective fabric must act as a particulate filter. The Individual Protective Equipment (IPE) fabric studied for this research consists of an outer tightly woven layer backed by an activated carbon inner layer, which is designed to filter out harmful vapors. The fibers, primarily in the outer woven layer of fabric, provide majority of the air flow resistance and particulate filtration. The interaction of the IPE fabric with particles is similar to that of filter media and, thus, traditional filtration theory can be used to analyze the performance of IPE fabric in filtering out particles directed towards them.

Although aerosol filtration is an extremely important factor pertaining to the design of the IPE fabric, little research has been performed to quantify the filtration performance of this material. The man-in-stimulant test (MIST) (reference 1) tests the entire IPE system on a person, simulating a real life scenario. The MIST procedure is an overall IPE performance standard; subsystem tests, also known as component tests, are, however, needed to quantify the performance of individual pieces of the IPE for design analysis. Previously, swatch tests were used to quantify aerosol penetration of IPE fabric (reference 2). In a swatch test, a piece of fabric is placed in a closed environment and air is forced through the material. The drawback of this method is that in a real world environment, air has the ability to flow around and is not forced though the fabric.

Here we present a simple approach to model the filtration characteristics of a component and establish an experimental method to test component performance. Three main sets of experiments were performed to aid development and testing of the component particle penetration model; a bench top filter holder test to establish the filtration efficiency and permeability of the IPE fabric; a swatch test to determine the performance of the fabric piece in a wind tunnel; and finally a sleeve component test to validate model predictions.

MODELING APPROACH

An IPE system must provide protection for an individual from airborne agents under a range of wind conditions. A full IPE system may be composed of individual components or subsystems such as, body suit, face mask, gloves, etc. as illustrated in Figure 1. A capability to predict the protective ability of the entire IPE system as a function of the IPE fabric material and ambient conditions will help determine the threat-level to an individual or group on exposure to airborne agents. Also, such a capability will enable optimization of the design of the components or their fabric material properties for best protective performance.

In this study, particle penetration characteristics of a sleeve component as a function of the directed ambient wind speed is investigated (illustrated in Figure 1). To model this system, the sleeve is idealized as a rigid, permeable cylinder, and the appendage on the inside as a solid cylinder. The component test is modeled in two steps. First, the flow through the fabric caused by the wind is predicted as a function of the angular (θ) locations. From the prediction of the local normal velocity (i.e., face velocity at any, angular location, $V_f(\theta)$), particle penetration is

estimated as a function of particle diameter using filtration theory. This approach is consistent with that of nonuniform filtration theory of Dhaniyala and Liu (references 3 and 4).

If fabric deformation can be ignored, potential flow assumption can be used to determine static pressure on the fabric surface of the simple cylindrical sleeve component geometry flow [$P_o(\theta)$]. To relate the flow inside the fabric sleeve to the external pressure distribution, the flow in the gap (ΔR) between the fabric and the inner cylinder is assumed to have a parabolic flow profile, and from mass conservation for the flow through the fabric and the flow in the gap and considering momentum conservation along the θ direction, the following equation are obtained:

$$\frac{d^2 P_i(\theta)}{d\theta^2} - \beta^2 P_i(\theta) = -\beta^2 P_0(\theta) \tag{1}$$

$$\beta^2 = \frac{12\mu\alpha R^2}{\Delta R^2} \tag{2}$$

where $P_i(\theta)$ is the pressure inside the fabric, μ is gas viscosity, α is fabric permeability, and R is the radius of the fabric cylinder. This formulation is based on the approach of Li, Liu, and Cheng (reference 5) and is illustrated in Figure 2. The pressure drop across the fabric at circumferential location θ is obtained as:

$$P_o(\theta) - P_i(\theta) = \frac{4\rho V_\infty^2 \cos 2\theta}{\beta^2 + 4} \tag{3}$$

where V_∞ is the freestream velocity, and ρ is the gas density.

To calculate air flow characteristics through and around the component test geometry, flow simulations using a computational fluid dynamics (CFD) approach can be used. Such simulations will help account for complex geometries and a range of media properties. But such simulations are complicated and will require significant computational time.

CFD calculations using the software FLUENT 6.3.26 (Fluent Inc., NH) were used to test the predictions of the simple potential flow model. In the CFD simulations, a porous jump boundary condition was used to represent the fabric media, and the component was located in a wind tunnel with velocity inlet and outflow conditions at the entrance and exit, respectively. The permeability of the media is a required input for the porous jump boundary, and this was obtained from experimental measurement of fabric pressure drop as a function of face velocity, as described in later.

The pressure drop (P_o–P_i) across the fabric at four different freestream velocities calculated using the potential flow model is compared with CFD simulations in Figure 3. For angles smaller than ~ 50 deg on the upstream side of the cylinder, the flow is seen to enter the component and for these angles, the potential flow and CFD results are largely in reasonable agreement

(Figure 3). The differences in pressures predicted by the different models are insignificant with respect to particle penetration calculation. The maximum pressure drop, and hence flow rate, is at the front of the fabric cylinder due to the dynamic pressure component of the freestream flow. For angles larger than 50 deg (i.e., where flow exits the component) the potential flow predictions begin to differ from CFD results. As penetration predictions only require accurate characterization of flow entering the component, the potential flow model should suffice for this case.

The component particle penetration model is developed by combining potential flow calculations with a particle filtration model. In this approach, bench top tests are used to obtain particle penetration data for the fabric media of interest for a range of operating conditions. From classical filtration theory, we obtain the single fiber filtration efficiency (E_Σ) as (reference 6):

$$E_\Sigma\left(V_f, D_p\right) = 1 - \left[(1 - B_1E_R)(1 - B_2E_I)(1 - B_3E_D)(1 - B_4E_{DR})\right] \tag{4}$$

where, V_f is face velocity, D_p is particle diameter, $B_{1\text{-}4}$ are media-dependent constants, E_R, E_I, E_D, and E_{DR} (Equation 5) are filtration efficiencies due to interception (reference 7), impaction (reference 8), diffusion (reference 6), and diffusion-enhanced interception (reference 7), E_Σ is the net single fiber filtration efficiency. The single fiber efficiencies due to the different mechanisms are calculated as:

$$\left.\begin{aligned} E_D &= 1.5Pe^{-2/3} \\ E_I &= \frac{Stk^2}{\left(1 + 0.55Stk\right)^2} \\ E_R &= \frac{1}{2Ku}\left[2(1+R)\ln(1+R) - (1+R) + (1+R)^{-1}\right] \\ E_{DR} &= \frac{1.24R^{2/3}}{(KuPe)^{1/2}} \end{aligned}\right\} \tag{5}$$

where Pe is the Peclet number, Stk is particle Stokes number, R is the interception parameter, and Ku is the Kuwabara constant. The interception parameter is the ratio of the particle diameter to the fiber diameter, while the Kuwabara constant (reference 9 and reference 10) is calculated as:

$$\mathrm{Ku} = \alpha - \frac{\left(\alpha^2\ 2\ln\alpha + 3\right)}{4}. \tag{6}$$

The total filter efficiency (η) can then be calculated as:

$$\eta = 1 - \exp\left(\frac{-4\alpha E_\Sigma t}{\pi d_f}\right) \tag{7}$$

where α is packing density, t is the media thickness and d_f is the average fiber diameter of the filter media.

Flow through woven media has often been modeled on two different fiber scales, the multifiber yarns and the intrayarn fibers. References 11, 12, and 13 all model flow through the fabric with varying pore sizes. The filtration model of reference 14, uses two different single fiber efficiencies for the yarn and the fibers. The IPE material is, however, very tightly woven, making any flow between the yarns negligible and the entirety of the flow can be assumed to pass through the yarns and between the fibers (reference 15). For the fabric media under test, an estimate of the fiber diameter is obtained from SEM analysis. Based on the measured fiber diameter, the packing density (α) can be calculated using fabric permeability (reference 6), or other theoretical approaches (e.g., reference 16). For known fabric media properties, the constants $B_{1\text{-}4}$ can be calculated from bench top experimental results of fabric penetration as a function of particle size and face velocity using a multivariate analysis. Thus, an expression for the net filter efficiency or penetration can be obtained as a function of particle size and flow velocity for a selected media.

The local pressure drop across the fabric located on the cylindrical component holder can be calculated using the potential flow model and the local face velocity [$V_f(\theta)$] can be obtained from the pressure drop calculations assuming constant local media permeability. For uniform upstream particle concentration, the net particle penetration through the component (1-η) can then obtained as the ratio of net particle flux passing through the fabric media to the particle flux directed towards the component holder:

$$penetration = \frac{\int_{\theta_1}^{\theta_2} \left(1 - \eta\ \left(V_f(\theta), D_p\right)\right) V_f(\theta) A(\theta)\ d\theta}{\int_{\theta_1}^{\theta_2} V_f(\theta) A(\theta)\ d\theta} \tag{8}$$

where θ_1 and θ_2 are the angles corresponding to the limits of the region through which the flow enters the cylindrical component. In Equation (8), the numerator represents the net particle penetration flux accounting for local filtration efficiencies and local flow flux. For a selected particle diameter and a known local velocity, the local penetration $[1 - \eta(V_f(\theta), D_p)]$, is obtained from bench top measurements of fabric efficiency (Equation 7). The net penetration can be calculated for varying face velocities and particle sizes and compared to experimental results.

EXPERIMENTAL PROCEDURE

BENCH TOP TESTS

To develop the fabric filtration model described above, bench top penetration data is needed to derive variables $B_{1\text{-}4}$ in Equation (4). A schematic diagram of the experimental setup used for these tests is shown in Figure 4. Aerosol particles were generated by nebulizing a solution of dioctyl sebacate (DOS) in isopropanol. The aerosol particles were passed through a desiccant dryer and into a 5-gal mixing chamber. In the mixing chamber, clean air was introduced to dry the aerosol and dilute the concentration. The large volume of the mixing chamber allows for temporal stability of the aerosol source, which is critical for accurate penetration measurements. After exiting the mixing chamber, the aerosol is passed through a Kr-85 neutralizer (TSI 3077) to charge-neutralize the particles before they are passed to the filter holder. The test fabric is located in the 47 mm filter holder, and penetration measurements are obtained from particle concentration measurements made upstream and downstream of the fabric. Particle concentrations were measured using two instruments: a scanning mobility particle sizer (SMPS) for particles in a size range of 10-500 nmi; and an aerodynamic particle sizer (APS; TSI 3321) for particles in the size range of 500 nmi to 2 μm. Face velocity through the fabric was controlled using a volume flow controller and a vacuum pump downstream of the filter holder. The pressure drop across the filter was monitored to ensure that the filter was not loaded during the measurements.

The experimental setup shown in Figure 4 is used for both penetration and permeability measurements. To measure penetration, upstream and downstream particle concentration measurements are made as a function of particle size and face velocity. For the permeability measurements, the aerosol generation and sampling systems are removed from the setup and only the differential pressure is monitored with varying flow rates trough the filter holder. The fabric permeability is determined from pressure drop measurements across the fabric as a function of face velocity.

SWATCH TESTS

Prior to running a full component test in the wind tunnel, it was critical to validate the performance of the wind tunnel aerosol injection and sampling systems. For this, a small piece of fabric (swatch) was located perpendicular to the flow in the tunnel cross-section, upstream of a chamber that is designed to control the face velocity through the fabric. This test, called the swatch test, is similar to the bench top experiments with the face velocity through the fabric being controlled with a pump rather than the wind. Consistent results with the swatch-holder and the bench top experiments will provide confidence on the wind tunnel injection and sampling systems.

A schematic diagram of the experimental setup used for the swatch tests is shown in Figure 5. Similar to the bench top experiments, test aerosol particles are generated using nebulizers. Four nebulizers are used in parallel to ensure that sufficient particle number concentrations in the tunnel for penetration measurements. A mixing chamber is used to ensure temporal

concentration uniformity of the generated aerosol. Particles are injected into the wind tunnel using an array of 12 injection ports, spread over an area of 3 in. x 3 in. The injection grid is covered with a coarse screen to facilitate turbulent mixing, and hence spatial uniformity, of the injected aerosol in the wind tunnel. The particles are then carried to the swatch by the wind, and particle concentrations upstream of the fabric holder are measured using a ¼ in. O.D. stainless steel tube placed ½ in. in front of the swatch.

The swatch holder consists of a 3 ft long, 3½ in. I.D. tube with the fabric sample attached at the front of the holder. Internal circumferential pressure ports allow monitoring of pressure drop across the fabric, to ensure that particle loading is not a factor in the penetration measurements. At the rear of the swatch holder a vacuum pump is connected to draw a required flow rate consistent with the desired face velocity. For downstream concentration measurements, flow is sampled from inside the swatch holder using a ¼ in. O.D. sample tube 6 in. downstream of the swatch. Subsequent testing revealed that the exact location of the downstream sample port inside the swatch holder was not important in determining downstream concentrations. Similar to the bench top test, upstream and downstream particle size distributions are measured using either an SMPS or an APS.

COMPONENT TESTS

The wind tunnel aerosol generation and sampling systems for the component tests were identical to that used in the swatch tests. The component holder consists of a cylindrical fabric sleeve holder of $4^{3}/_{8}$ in. diameter, which is the standard sleeve size for the IPE, surrounding a solid inner cylinder of diameter 3¼ in., representing a human arm (Figure 6). In the component holder, two sampling tubes are located in the $^{9}/_{16}$ in. gap between the cylinders for particle concentration measurements – one flush with the inner cylinder surface and the other located midpoint between the inner cylinder and the fabric. These sample tubes are used to determine the effect of radial sampling location on the measurement of downstream particle concentration. Pressure measurement ports are also located just inside and outside of the sleeve for pressure drop measurements. The pressure ports are oriented vertically, flush against the fabric to measure static pressures at the desired locations. The pressure drop measurements across the fabric are used to calculate local face velocities for varying ambient wind conditions and angular positions on the fabric cylinder.

In realistic scenarios, the fabric sleeve will deform and flutter. Particle penetration through a fabric sleeve under those conditions is a combination of the spatial and temporal distribution of penetrating flow fields and the resulting particle paths. While the eventual goal is to model such a system, a preliminary model that explains the interaction of ambient wind and particle paths must be established first. To prevent fabric deformation and fluttering at high wind speeds, a support screen just inside the fabric sleeve cylinder is used (Figure 7). This artificial constraint on the fabric geometry provides a simple baseline case for comparison of experiment results with the CFD and potential flow modeling predictions. To eliminate any 3-D flow effect in the wind tunnel, the stand at the bottom of the component holder was also covered with a fabric and a support screen (Figure 7).

To determine the effect of the support screen and the bottom sleeve covering the stand, pressure drop measurements were made across the fabric at the front of the cylinder ($\theta = 0$ deg) for different configurations (Figure 8). The presence of the screen and extension of the sleeve over the entire height of the cylinder is seen to result in pressure drop measurements that match modeling results. Penetration measurements were then made with this configuration for a range of wind speeds and particle sizes.

THIS PAGE INTENTIONALLY LEFT BLANK

RESULTS AND DISCUSSION

BENCH TOP TESTS

Bench top filter holder tests were performed at four different fabric face velocities, ranging from 6.5 cm s^{-1} to 27 cm s^{-1}. The range of face velocities represents the limits of the experimental setup. The minimum flow rate required by the sampling instruments (without external dilution for measurements) resulted in the minimum face velocity of 6.5 cm s^{-1}, and for face velocities greater than 27cm s^{-1}, the pressures in the filter holder were too low for the sampling instruments. The penetration measurement results for the four different face velocities are plotted in Figure 9. The error bars in Figure 9 represent the range of penetration values for five different fabric pieces. From the general shape of the penetration curves, it is seen that the IPE fabric behaves similar to traditional filtration media (reference 17).

Increasing the face velocity increases the penetration at small particle diameters, while decreasing the penetration of larger particle diameters. This occurs because increasing the face velocity decreases particle capture by diffusion, permitting more small particles to pass through. Higher face velocities increase particle stokes number, and thus enhance particle capture by inertial impaction particularly for larger particles which have sizes corresponding to the inertial regime (Stokes number > ~ 1). Based on least squares analysis of the bench top experimental data, the expressions for variables $B_{1\text{-}4}$ were obtained as:

$$\left.\begin{aligned} B_1 &= 0.2; \\ B_2 &= 12.28; \\ B_3 &= 15(V_f^2) - 5.8V_f + 0.56 \quad \text{for } 0 < V_f < 0.2 \text{ ms}^{-1}; \\ &= 0.01; \quad\quad\quad\quad\quad\quad\quad\quad\quad\quad\quad\quad \text{for } V_f > 0.2\text{ms}^{-1} \\ B_4 &= 7.9V_f + 0.54; \end{aligned}\right\} \tag{9}$$

The variables B_3 and B_4 are dependent on face velocity. Combining Equations (4) and (7), particle penetration through a selected fabric media can be expressed as a function of particle diameter and fabric face velocity. A simple comparison of the predictions of the fabric penetration model with the bench top experimental data for the four different face velocities is shown in Figure 10. As expected, the filtration model agrees well with the experimental data that were used to generate the model.

The contributions of diffusion, interception, and impaction on the total single fiber efficiency of the fabric media is illustrated in Figures 11 and 12. For a low face velocity (6.5 cm s^{-1}), diffusion is the main capture mechanism for small particles and interception is the main mechanism for large particles. When the face velocity is increased to 27 cm s^{-1}, the Stokes number increases and impaction plays a much larger role.

SWATCH TESTS

The swatch tests were conducted to establish the wind tunnel injection and sampling systems, and to investigate if fabric penetration characteristics at a constant face velocity was independent of freestream velocity. Initial penetration tests were performed at near isokinetic conditions with no swatch (fabric) in the swatch holder. The objective of this test was to confirm that a penetration of 100% was obtained, for validation of our upstream and downstream measurement systems. Because of limits on the vacuum pump and the wind tunnel, exact isokinetic conditions could not be achieved. The vacuum pump was able to provide a maximum swatch holder face velocity of approximately 0.3 m/sec, and the wind tunnel was able to provide a minimum stable freestream velocity of 0.6 m/sec (2 ft/sec). In these experiments, for 15 particle diameters ranging from 30 to 300 nmi, an average penetration of 0.97 with a standard deviation of 0.04 was observed. This provides initial validation of the measurement and injection systems in the wind tunnel.

The next tests were with the swatch in place at the entrance of the swatch holder. The swatch penetration measurement results for two different freestream wind speeds (30 and 60 ft/sec) are shown in Figure 13. Also shown in Figure 13 are bench top results for the equivalent face velocity (27 cm s^{-1}). The results suggest that there is no discernible effect of freestream wind velocity on particle penetration when the fabric face velocity is constant. The independence of penetration on freestream velocity is consistent with the small Stokes numbers of the test particles, calculated based on the fiber diameter. The swatch-holder test results, therefore, provide an initial validation of the wind tunnel injection and sampling systems.

COMPONENT TESTS

The LLC potential flow model is used to determine face velocities through the component cylindrical fabric sleeve as a function of angular position, and the face velocities are combined with the filtration model to determine the net particle penetration (Equation (8)) through the component at a function of freestream velocity. The model predictions of particle penetration for the component model are shown in Figure 14 for four freestream velocities ranging from 30 to 120 ft/sec.

Particle penetration characteristics of the IPE component sleeve depend significantly on freestream velocities. At low wind speeds, the diffusional capture mechanism dominates and particles smaller than 50 nmi are efficiently captured, but larger particles (~ 1 μm) penetrate through the fabric as they are not effectively captured either by diffusion or inertial impaction. Particles larger than 2 μm are effectively captured by the IPE fabric over the entire range of wind speeds studied (30-120 ft/sec) due to their large size and Stokes numbers. Particles 2 μm and larger are efficiently captured by interception and impaction. As wind speeds are increased, the inertial capture of particles shifts to smaller sizes. At high wind speeds, however, the residence time of particles in the region closest to the fibers is reduced, and thus diffusional capture efficiency decreases. For the fabric media studied, the model suggests that peak particle penetration occurs for wind velocity in the range of 90 to 120 ft/sec. However, considering the

air flow rate through the fabric, the total particle flux passing through the fabric increases with increasing wind speed.

To validate the results of the model, penetration measurements of the component sleeve were made at freestream velocities of 30, 60, 90, and 120 ft/sec in the wind tunnel. For valid experimental results, it is important to ensure that the flow flux and particle penetration through the component fabric is only dependent on the ambient wind velocities and not on the sampling flow rate of the particle instruments downstream of the swatch. For this, penetration measurements were obtained with different flow rates through the downstream sample probe and it was observed that there was no change in particle concentrations downstream of the fabric, suggesting that the instrument sample flow rates were significantly smaller than the ambient wind-driven flow flux. The effect of the θ-location of the downstream sampler was also investigated. It was found that the location angle of the sampler made a difference in the measurement of downstream particle concentration, suggesting the air volume between the outer fabric cylinder and the inner cylinder is not well mixed. As there are no mechanisms inside the component holder that will result in an enhancement of concentration, the final location of the probe was chosen based on the location that yielded the maximum penetration value (θ = ~ 30-60 deg). The experimental data plotted with the penetration predicted by the model at 30, 60, 90, and 120 ft/sec are shown in Figures 15 through 18, respectively. The error bars in the plots represent the standard deviation of the obtained results with three different sleeves.

The error bars for penetration measurements are larger for small particles due to the choice of generated aerosol size distribution and the measurement technique. To ensure sufficient aerosol concentration over the entire test size range, the test aerosol was generated with a mean size ~ 300-500 nmi, resulting in fewer particles in the smaller size range. Also, for fast measurement, the SMPS scan time was set to 2 min and 10 diameter channels, resulting in only a 12-sec sampling time per diameter channel. For larger particles, measurement with the APS was made over a 1-min interval, resulting in better counting statistics of these particles. The error estimates based on counting statistics were also consistent with the variability in the measurements.

Over the entire size range, the experimental results compared well with the predictions of the component penetration model that was obtained by combining the potential flow and the filtration models. As predicted, because of diffusional capture, particle capture efficiency was greater at lower wind speeds. Maximum penetration was seen to occur at a wind speed of 90 ft/sec, with capture by impaction causing the penetration to decrease from 90 to 120 ft/sec.

THIS PAGE INTENTIONALLY LEFT BLANK

CONCLUSIONS

The use of IPE for protection against particle exposure requires the knowledge of their performance over a range of operating conditions. Here, we present a simple approach to model the performance of an IPE fabric component as a function of particle diameter and directed wind velocity. Bench top experiments suggest that the IPE fabric behaves like standard filtration media, and that its performance can be modeled using traditional single fiber efficiency equations. The nonstandard characteristics of the fabric, such as the woven structure and the multiple layers, are accounted for as media-specific parameters in the penetration equation, which can be determined from simple bench top experiments. For experimental tests of the IPE component performance, a wind tunnel aerosol injection system was developed and this system was seen to provide temporally and spatially uniform particle concentration in the test section, which allowed for accurate penetration measurements.

A component sleeve model was developed by combining a potential flow model with nonuniform filtration theory. The flow model is simple and idealized, and is used to determine local pressure drops, and hence local face velocities, across the cylindrical component fabric sleeve based on experimentally-determined permeability values. The nonuniform filtration model, with parameters obtained from a small number of bench top experiments, can then be combined with the potential flow model to calculate net particle penetration through the component fabric sleeve caused by ambient winds. The model predictions of particle penetration through a component sleeve, as a function of particle size and face velocity, are seen to match well with wind tunnel measurements. The experimental and theoretical approaches can be extended to characterize particle penetration through full suit IPE systems.

THIS PAGE INTENTIONALLY LEFT BLANK

REFERENCES

1. U.S. Army Dugway Proving Ground: *Final Report for the Development of the Man-in-Simulant Test (MIST) Methodology for Evaluation of Chemical/Biological (CB) Protective Garments.* TECOM project No. 8-EI-825-ABO-004, Dugway, Utah, 1996.

2. U.S. Army Dugway Proving Ground: *Permeation of Air-Permeable, Semipermeable and Impermeable Materials with Chemical Agents or Simulants (Swatch Testing).* TOP 8-2-501, Dugway, Utah, 1997.

3. Dhaniyala, S. and Liu, B.Y.H., "Experimental Investigation of Local Efficiency Variation in Fibrous Filters," *Aerosol Science and Technology*, 34 (2), pp. 161-169, 2001.

4. Dhaniyala, S. and Liu, B.Y.H., "Theoretical Modeling of Filtration by Nonuniform Fibrous Filters," *Aerosol Science and Technology*, 34 (2) pp. 170-178, 2001.

5. Li, L., Jiangge L., and Daiyun C., "Aerodynamic Adsorption of Permeable Chemical Protective Suit," *American Industrial Hygiene Association Journal* 62, pp. 559-562, 2001.

6. Davies, C. N. Air Filtration. New York: Academic Press, ISBN 0-12-205660-4, 1973.

7. Stechkina, I. B., and Fuchs, N. A., "Studies on Fibrous Aerosol Filters— I. Calculation of Diffusional Deposition of Aerosols in Fibrous Filters," *Annals of Occupational Hygiene*, *9*, pp. 59–64, 1966.

8. Langmuir, I., "The Production of Rain by Chain Reaction in Cumulus Clouds at Temperatures Above Freezing," *International Journal of Meteorology*, *5*, pp. 175–192, 1948.

9. Liu, B.Y.H., Rubow, K.L. and Pui, D.Y.H., "New Concepts in Aerosol Filtration: Experimental Studies and Filter Media Evaluation*", U.S. Army Chemical Research, Development and Engineering Center Conference on Chemical Defense Research,* Aberdeen Proving Ground, Maryland, 17-21 Nov 1987.

10. Matteson, M.J., and Orr, C., Filtration: Principles and Practices, Marcel Dekker, Inc., New York, 1987.

11. Goodings, A.C., "Air Flow through Textile Fabrics," *Textile Research Journ*al, 34, pp. 713-724, 1964.

12. Breard, J., Henzel, Y., Trochu, F., Gauvin, R., "Analysis of Dynamic Flows Through Porous Media. Part I: Comparison between Saturated and Unsaturated Flows in Fibrous Reinforcements," *Polymer Composites*, 24(3), pp. 391-408, 2003.

13. Wang, J., Chen, D.R., and Pui, D.Y.H., "Modeling of Filtration Efficiency of Nanoparticles in Standard Filter Media," *Journal of Nanoparticle Research*, 9, pp. 109-115, 2007.

14. Benesse, M., Le Coq, L., and Solliec, C., "Collection Efficiency of a Woven Filter Made of Multifiber Yarn: Experimental Characterization During Loading and Clean Filter Modeling Based on a Two-Tier Single Fiber Approach," *Journal of Aerosol Science* 37, pp. 974-989, 2006.

15. Gibson, P., Rivin, D., Kendrick, C., Schreuder-Gibson, H., "Humidity-Dependent Air Permeability of Textile Materials," *Textile Research Journal*, Vol. 69, No. 5, pp. 311-317, May 1999.

16. Dhaniyala, S. and Liu, B.Y.H., "An Asymmetric, 3-D Model for Fibrous Filters," *Aerosol Science and Technology* 30, pp. 333-348, 1999.

17. Dhaniyala, S., and Liu, B.Y.H., "Investigations of Particle Penetration in Fibrous Filters part I. Experimental," *Journal of the IEST* 42 (1), pp. 32-40, 1999.

APPENDIX
FIGURES

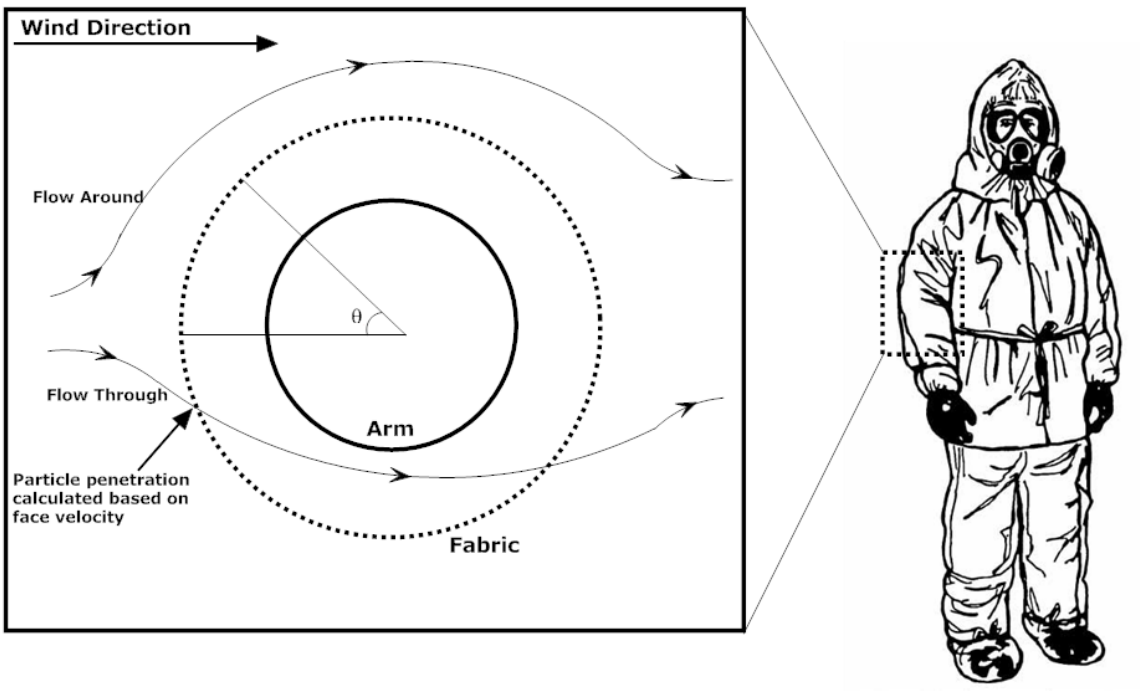

Figure 1: Approach to modeling the component test: the sleeve is modeled as a rigid permeable cylinder, with a solid inner cylinder representing an appendage.

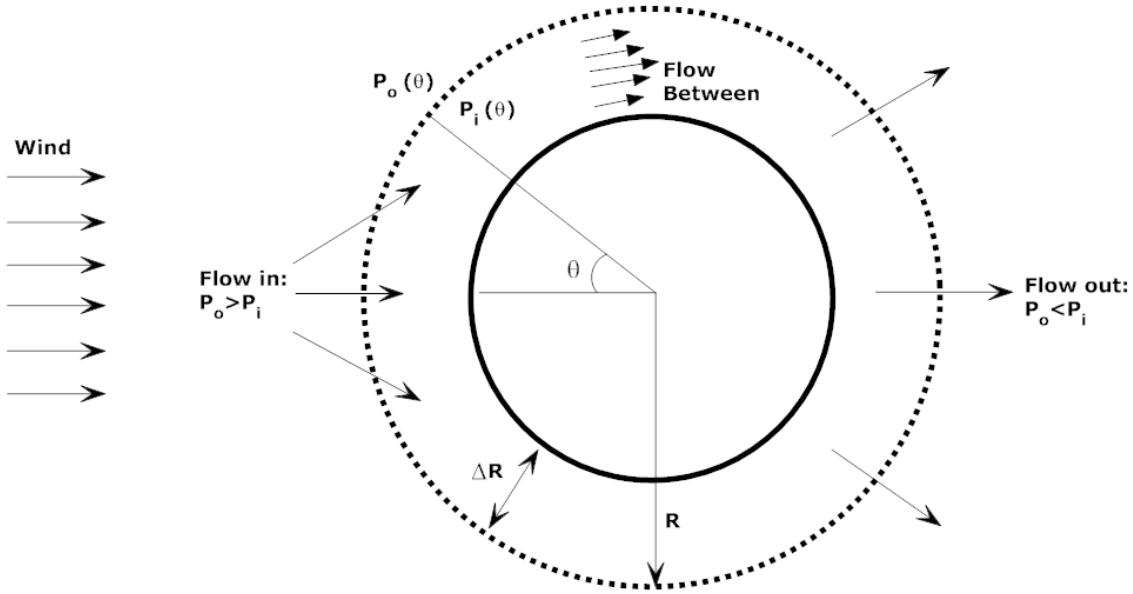

Figure 2: Illustration of the potential flow model from Li, Liu, and Cheng (2001).

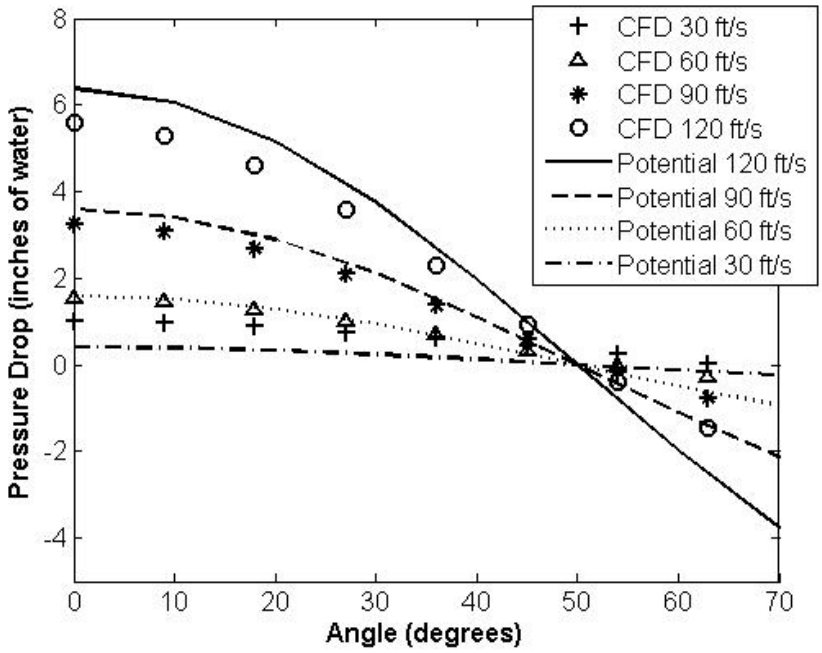

Figure 3: Pressure drop across fabric predicted by potential flow and the numerical model plotted at 4 different freestream velocity values.

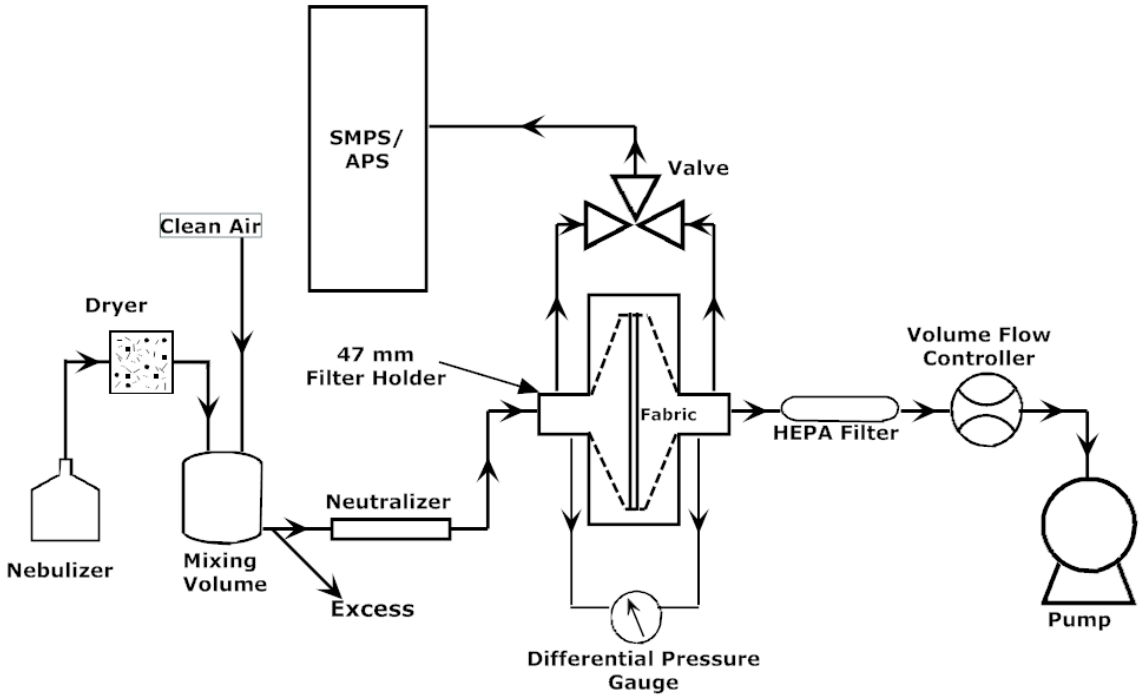

Figure 4: Schematic diagram of the bench top test setup used for fabric penetration measurements as a function of particle size and face velocity.

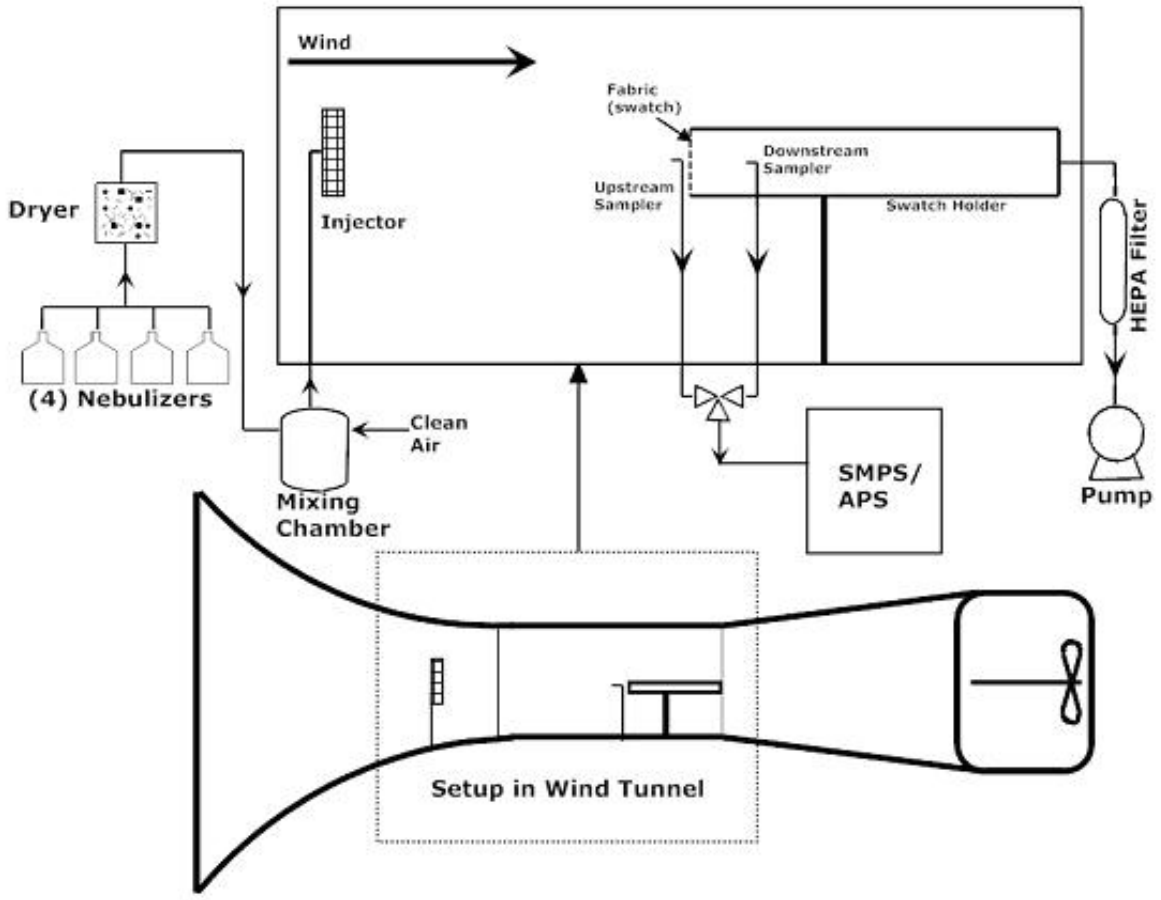

Figure 5: Swatch test setup in wind tunnel. The wind tunnel test section is 4 ft wide and 3 ft tall.

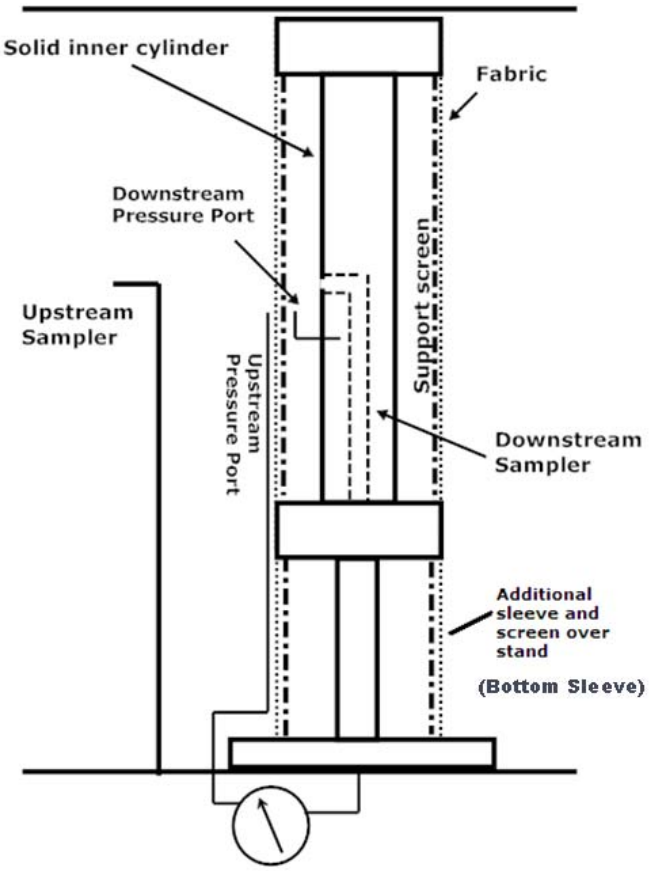

Figure 6: Component test setup. The wind tunnel injection and sampling system are identical to that of the swatch holder setup.

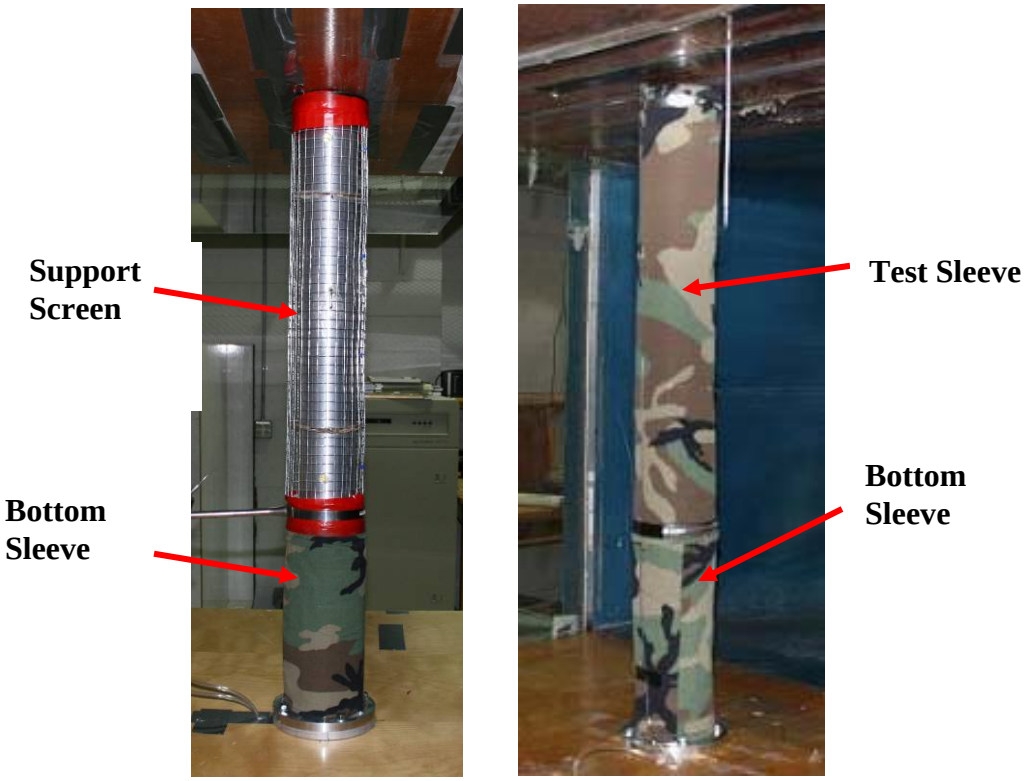

Figure 7: Component holder with fabric support screen and additional sleeve covering the stand at the bottom, and full component test with sleeve.

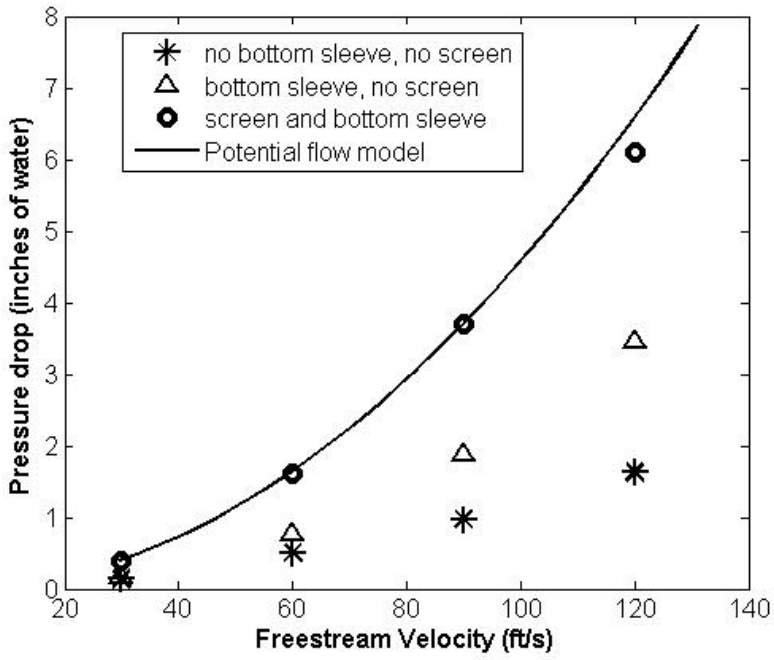

Figure 8: Pressure drop measurements at $\theta = 0$ compared to the potential flow model.

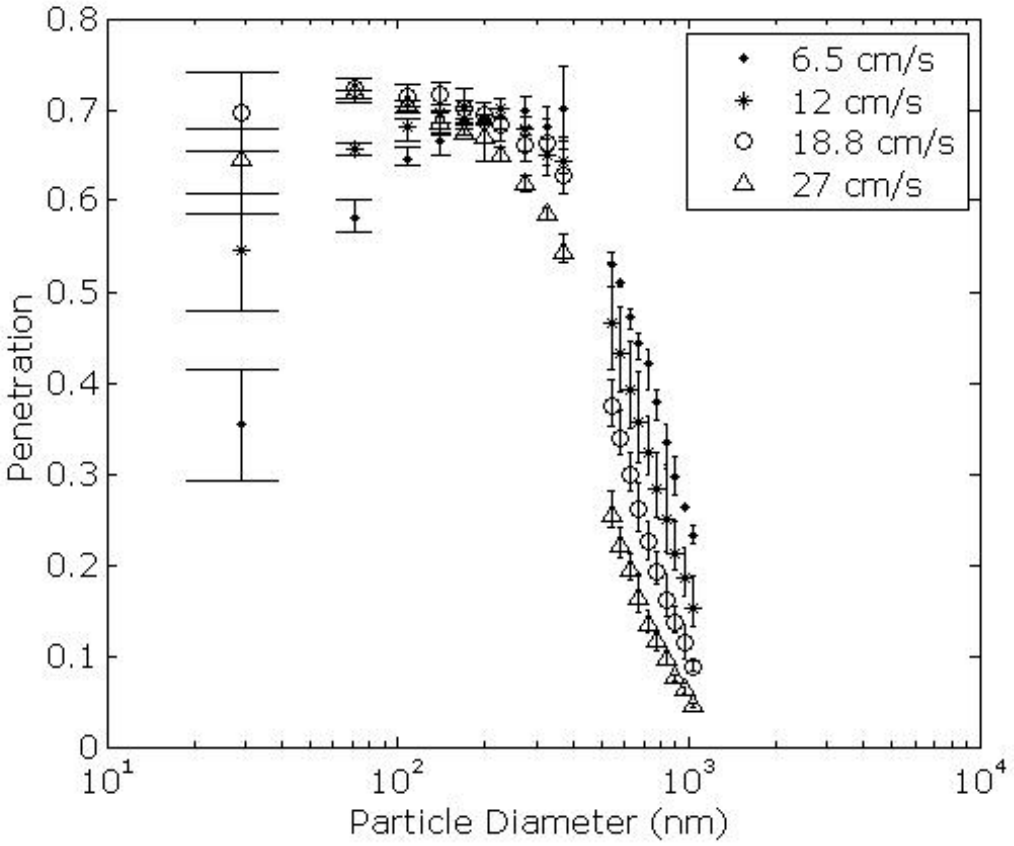

Figure 9: Bench top penetration results for four different face velocities. These values were used to find variables b_1-b_4 in Equation 4.

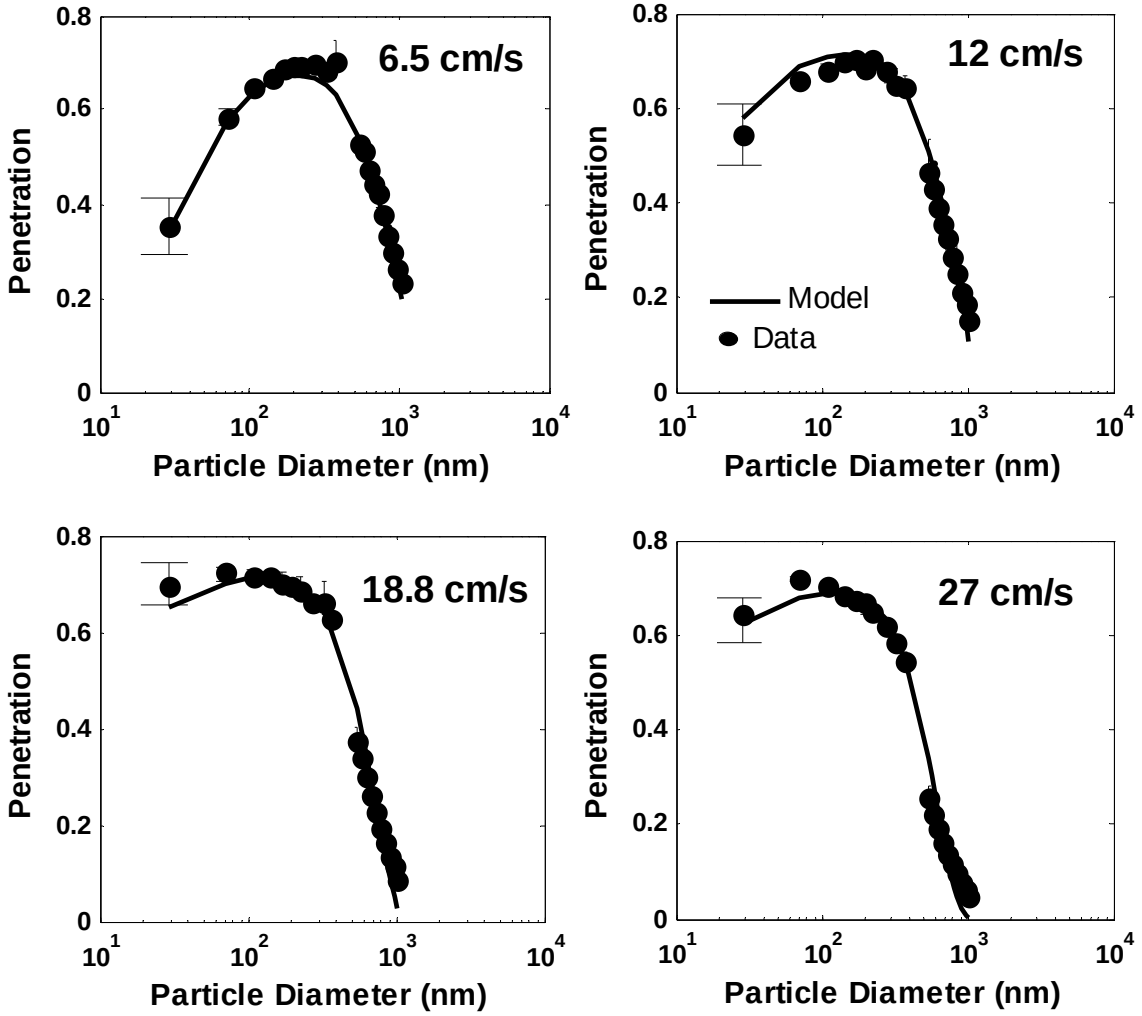

Figure 10: Filtration model plotted with experimental data at four face velocities.

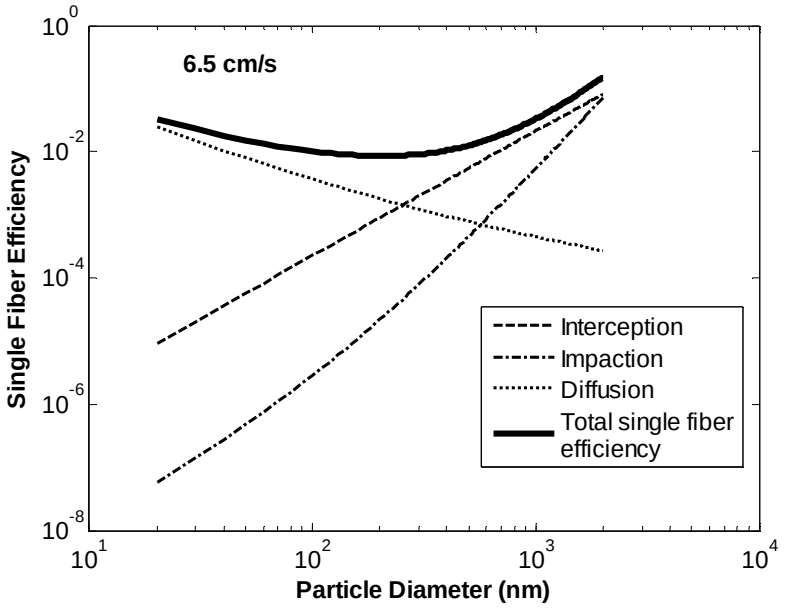

Figure 11: Contribution of filtration mechanisms for 6.5 cm s^{-1} face velocity.

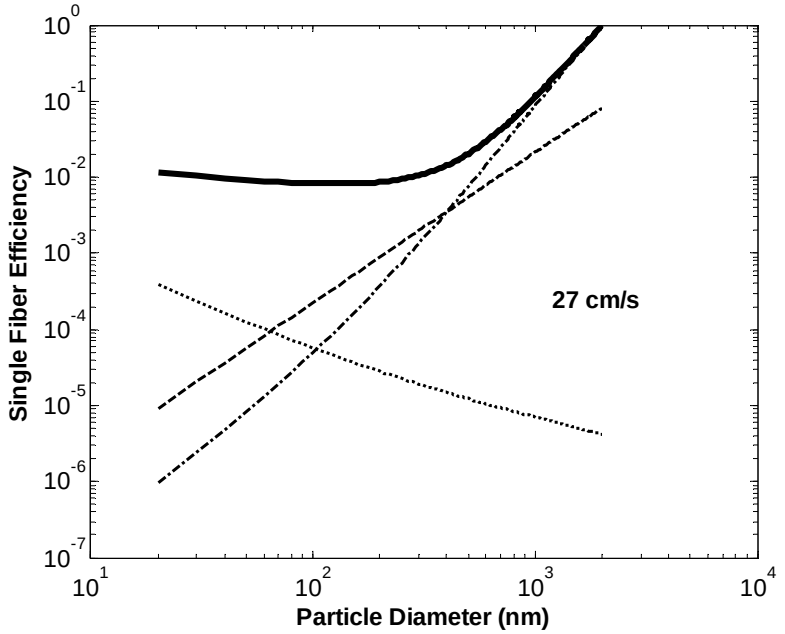

Figure 12: Contribution of filtration mechanisms for 27 cm s^{-1} face velocity.

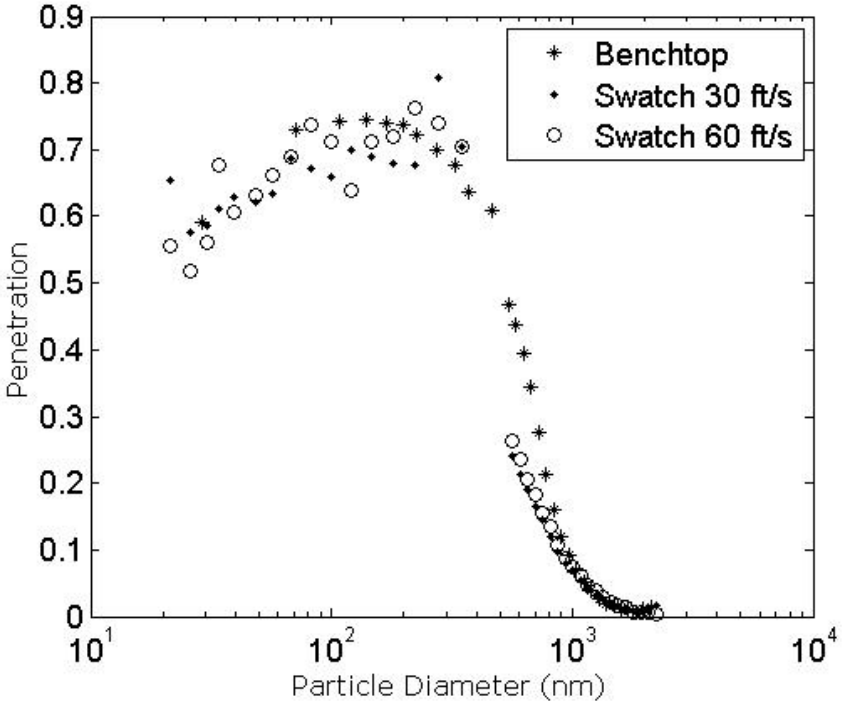

Figure 13: Wind tunnel swatch test results for 2 different freestream velocities plotted with bench top data of equivalent face velocity (27cm/s).

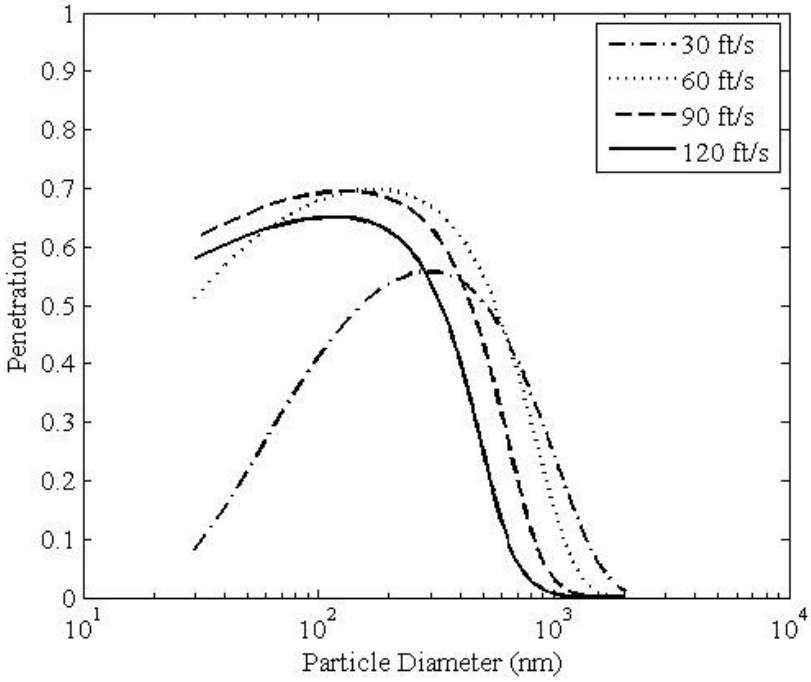

Figure 14: Component penetration predicted by the model.

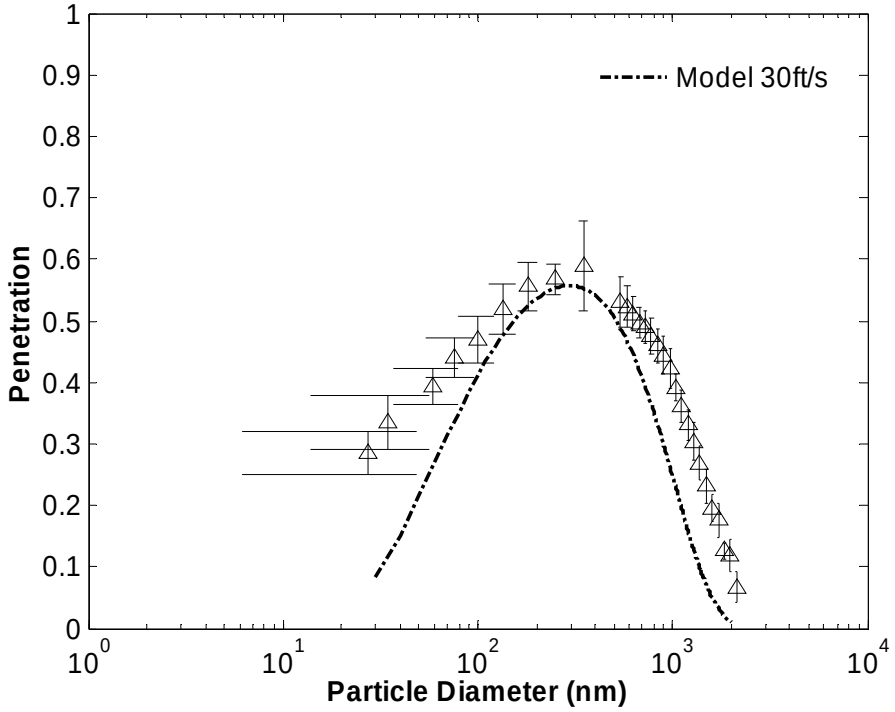

Figure 15: Penetration results for component test at 30 ft/sec wind speed.

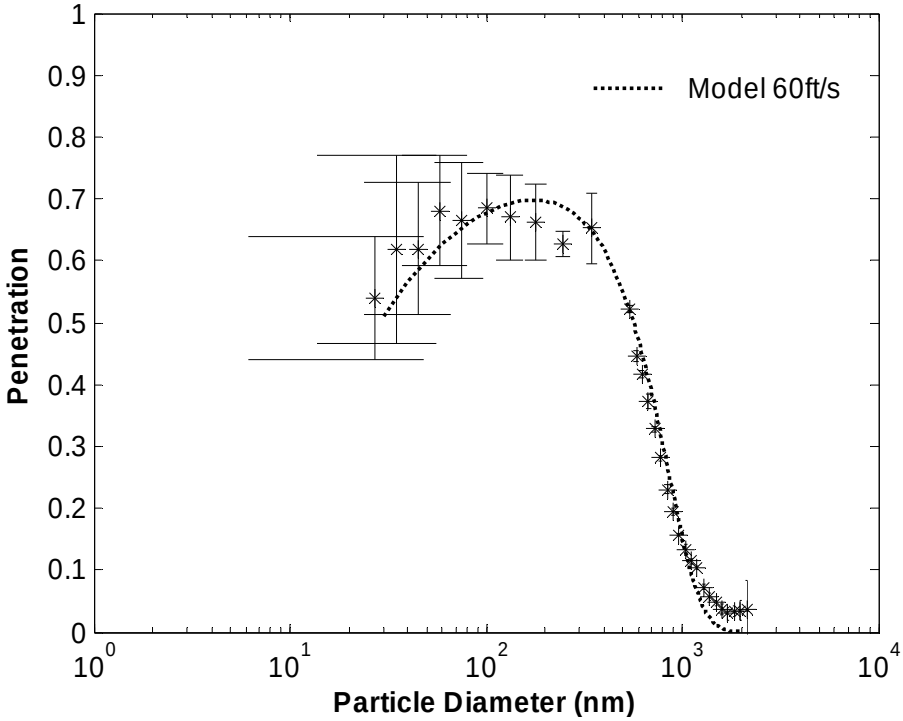

Figure 16: Penetration results for component test at 60 ft/sec wind speed.

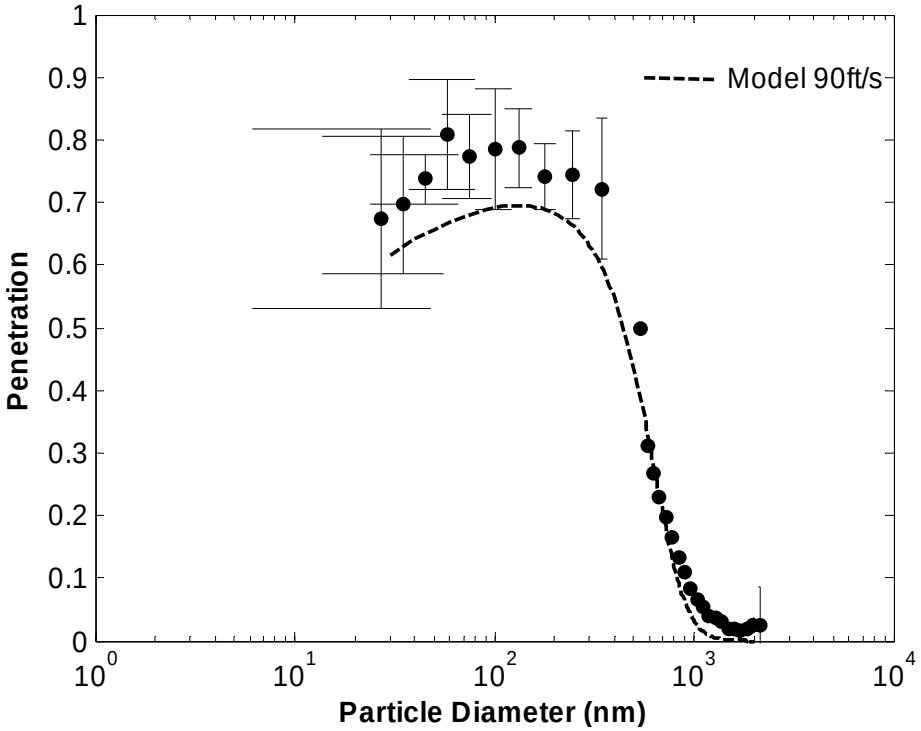

Figure 17: Penetration results for component test at 90 ft/sec wind speed.

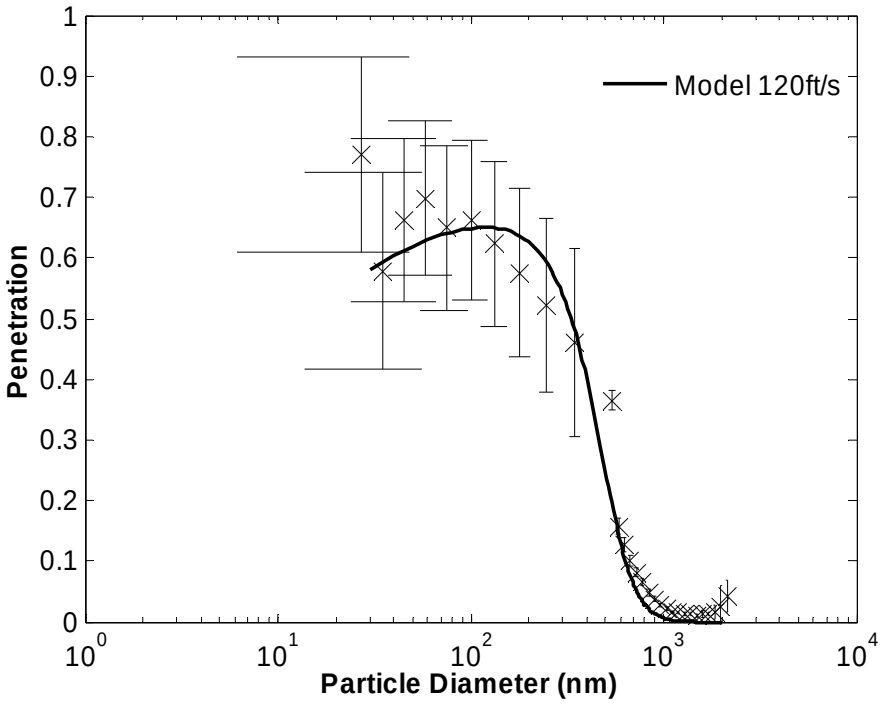

Figure 18: Penetration results for component test at 120 ft/sec wind speed.

DISTRIBUTION:

NAVAIRSYSCOM (4.3.2.1/Ghee), Bldg. 2187, Room 1320 (10)
48110 Shaw Road, Patuxent River, MD 20670-1906
NAVAIRSYSCOM (4.6.5.6), Bldg. 2187, Room 1320 (5)
48110 Shaw Road, Patuxent River, MD 20670-1906
Defense Threat Reduction Agency, JSTO CB/CBT (5)
8725 John J. Kingman Road, Ft. Belvoir, VA 22060-6201
NAVAIRWARCENACDIV (4.12.6.2), Bldg. 407, Room 116 (1)
22269 Cedar Point Road, Patuxent River, MD 20670-1120
DTIC (1)
8725 John J. Kingman Road, Suite 0944, Ft. Belvoir, VA 22060-6218